

Signatures of neutral quantum Hall modes in transport through low-density constrictions

Bernd Rosenow and Bertrand I. Halperin

Physics Department, Harvard University, Cambridge, Massachusetts 02138, USA

(Received 15 March 2010; published 19 April 2010)

Constrictions in fractional quantum Hall (FQH) systems not only facilitate backscattering between counter-propagating edge modes, but also may have a reduced constriction filling fraction ν_c with respect to the bulk filling fraction ν_b . If both ν_b and ν_c correspond to incompressible FQH states, at least part of the constriction region is surrounded by composite edges, whose low-energy dynamics is characterized by a charge mode and one or several neutral modes. In the incoherent regime, decay of neutral modes describes the equilibration of composite FQH edges, while in the limit of coherent transport, the presence of neutral modes gives rise to universal conductance fluctuations. In addition, neutral modes renormalize the strength of scattering across the constriction and thus can determine the relative strength of forward and backward scatterings.

DOI: [10.1103/PhysRevB.81.165313](https://doi.org/10.1103/PhysRevB.81.165313)

PACS number(s): 73.43.Cd, 73.43.Jn

I. INTRODUCTION

The strongly correlated nature of fractional quantum Hall (FQH) states is reflected in their unusual low-energy edge excitations. Edges of simple FQH states realize a chiral Luttinger liquid (LL) (Ref. 1), and backscattering between counterpropagating FQH edges can be used to study their dynamics. For FQH quasiparticles, the backscattering amplitude is then expected to increase with decreasing source-drain voltage, giving rise to a zero bias peak in the differential resistance. Scattering between FQH edges is facilitated by a constriction region, where two counterpropagating edges approach each other closely. Due to the confining potential, the constriction filling fraction ν_c is generally smaller than the bulk filling fraction ν_b , and interesting transport characteristics result.²⁻⁴ For $\nu_b=1$, a zero-bias peak in the differential resistance was experimentally observed for $\nu_c < 1/2$ while for $\nu_c > 1/2$ a zero-bias dip was seen instead^{3,4} and interpreted in terms of particle-hole transformations.^{4,5}

In this paper, we analyze charge transport through a low-density FQH constriction. If both ν_b and ν_c are incompressible states, the constriction region is surrounded by two types of edges: between ν_c and vacuum, and between ν_b and ν_c . At least one of these edges is a composite edge with counterpropagating modes. If spatially random intraedge scattering is relevant, the low-energy physics of composite edges is described by a random fixed point with a charged mode decoupled from one or several neutral modes.^{6,7} Interest in the physics of FQH neutral edge modes has been revived by the fact that the postulated non-Abelian statistics of the $\nu=5/2$ FQH state is encoded in a neutral Majorana mode.⁸

Edge equilibration is described by the decay of the neutral mode with a disorder-induced equilibration length ℓ . Denoting the geometric constriction size by L and the neutral mode velocity by v_σ , there are additional length scales $L_T = v_\sigma \hbar / k_B T$ determined by temperature and $L_V = v_\sigma \hbar / eV$ determined by the source-drain voltage. In the diffusive limit $\ell \ll L$ and $\min(L_T, L_V) < L$, transport through the constriction acquires a temperature and voltage dependence through the neutral-mode decay length $\ell(T, V)$. In the coherent limit $L_T, L_V > L$, $\ell < L$, neutral-edge modes have a dramatic influence on transport as they give rise to universal conductance

oscillations. The conductance through the constriction can take any value between zero and $\nu_b e^2/h$, and changes as a function of chemical potential or magnetic field.

If there is interedge scattering across the constriction, its strength is renormalized by the neutral-mode dynamics. In the idealized model of a fully equilibrated constriction in the diffusive regime, we calculate the scaling dimensions of the most relevant operators for backwards and forward scattering. If the bare scattering matrix elements for both processes are comparable, the renormalization determines which one is dominant and whether a zero-bias peak or zero-bias dip in the differential resistance is expected. For $\nu_b=1$, our calculation agrees with the result of the particle-hole transformation^{4,5} while we find a different result for some $\nu_b \neq 1$. We compare our predictions for zero-bias peaks and dips for different filling fractions with experiments. For the $\nu=5/2$ state, the non-Abelian neutral mode influences scattering across a constriction, and we find that for $\nu_b=3$ and $\nu_c=5/2$ the renormalization of scattering by the neutral mode may allow to distinguish the Pfaffian (Pf) state from its particle-hole conjugate partner, the anti-Pfaffian (APf).^{9,10}

II. DESCRIPTION OF LOW-DENSITY CONSTRICTION

We model the setup Fig. 1(a) by two chiral ν_b edges following paths C_1 and C_2 , and a closed ν_c edge surrounding the constriction region along a path C_3 . In the segments $C_1 \cap C_3$ and $C_2 \cap C_3$ two edge channels are in spatial proximity to each other, and are coupled both by a repulsive Coulomb interaction and scattering of charge e electrons. The imaginary time Lagrangians for this setup are

$$\begin{aligned} \mathcal{L}_0 = & \frac{1}{4\pi\nu_b} \sum_{\alpha=1,2} \int_{C_\alpha} dx \partial_x \Phi_\alpha (i\partial_\tau + v_b \partial_x) \Phi_\alpha \\ & + \frac{1}{4\pi\nu_c} \int_{C_3} dx \partial_x \Phi_3 (-i\partial_\tau + v_c \partial_x) \Phi_3, \end{aligned} \quad (1)$$

$$\mathcal{L}_{\text{int}} = \sum_{\alpha=1,2} v_{bc} \int_{C_\alpha \cap C_3} dx (\partial_x \Phi_\alpha) (\partial_x \Phi_3), \quad (2)$$

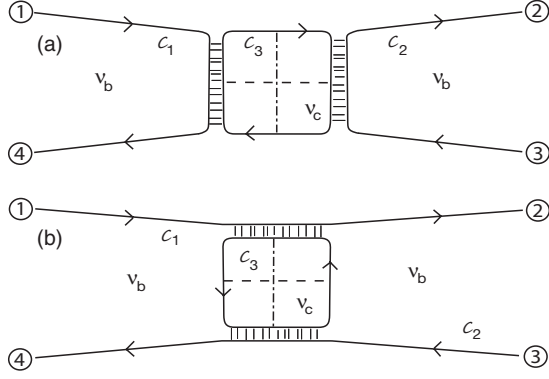


FIG. 1. Sketch of a Hall bar with a low-density region in a constriction. (a) Simple edges bulk vacuum and constriction vacuum, composite edges with two counterpropagating modes between bulk and constriction. In the lower panel (b), bulk-vacuum and bulk-constriction edges are simple while constriction-vacuum edges are composite. Thin full lines represent intraedge scattering, and dashed and dashed-dotted lines interedge scattering.

$$\mathcal{L}_{\text{scat}} = \sum_{\alpha=1,2} \int_{C_\alpha \cap C_3} dx [\xi(x) e^{i\Phi_\alpha/v_b + \Phi_3/v_c} + \text{c.c.}] \quad (3)$$

with C_3 defined in the counterclockwise direction. Here, \mathcal{L}_0 describes simple edges propagating with velocities v_b and v_c along contours C_i , $i=1,2,3$. For setup Fig. 1(b), C_3 is defined in the clockwise direction and the dynamics of Φ_3 is governed by the LL parameter $\nu_b - \nu_c$. The electron density on edge i is described by $\frac{1}{2\pi} \partial_x \Phi_i$. Interaction and scattering of electrons between the bulk and constriction edges are described by \mathcal{L}_{int} and $\mathcal{L}_{\text{scat}}$, respectively. $\xi(x)$ is a complex Gaussian random variable with mean zero and variance $\xi^*(x)\xi(x') = W_0 \delta(x-x')$. The disorder defines a bare equilibration length $\ell_0 \sim 1/W_0$.

To illustrate the influence of edge equilibration on transport properties, we first discuss a single composite edge. We define an edge conductance $G_{ab} = (\partial I_b / \partial V_a)|_{V_c}$, where I_b is the edge current at point b , and V_a and V_c are voltages at contacts a and c (see Fig. 2). Using G_{ab} , we then calculate the conductance G_{12} between contacts one and two of the constriction under the assumptions that the simple edges surrounding the constriction are in equilibrium and that current conservation $I_a + I_c = I_b + I_d$ holds for composite edges.

We first discuss the case $\nu_b = 1$, $\nu_c = 1/3$, and generalize to other ν_b and ν_c later. For this special choice of parameters, the interaction region between bulk and constriction edges is

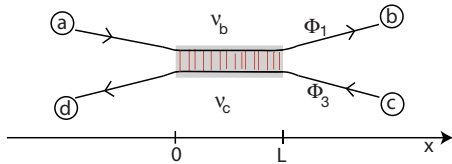


FIG. 2. (Color online) Sketch of the composite edge between a ν_b and ν_c incompressible quantum Hall regions. In the shaded contact region there is both interedge tunneling of electrons and a local Coulomb repulsion between counterpropagating edge modes.

equivalent to the composite $\nu = 2/3$ edge discussed in Ref. 6. In the following, we briefly summarize the main results of this reference. The disorder variance scales under a renormalization group (RG) transformation as $\frac{dW}{dl} = (3 - 2\Delta)W$. The scaling dimension Δ of the scattering operator Eq. (3) flows under the RG as well; it has the initial value $\Delta_0 = 2\sqrt{3}(v_b + v_c - v_{bc}) / \sqrt{3(v_b + v_c)^2 - 4v_{bc}^2}$. For $\Delta_0 < 3/2$, scattering between the two edges is relevant, and the RG flows to a fixed point characterized by $\Delta^* = 1$ and disorder strength W^* . At this random fixed point, the composite edge formed in the interaction region between fields Φ_1 and Φ_3 is described by a charge mode $\Phi_\rho = \Phi_1 + \Phi_3$ and a neutral mode $\Phi_\sigma = \Phi_1 + 3\Phi_3$, which are decoupled from each other. For $L \gg \ell$, the interacting region in Fig. 2 can be described by the fixed point Lagrangian

$$\mathcal{L}_{\rho\sigma}^* = \int_0^L dx \left[\frac{3}{8\pi} \partial_x \Phi_\rho (i\partial_\tau + v_\rho \partial_x) \Phi_\rho + \frac{1}{8\pi} \partial_x \Phi_\sigma (-i\partial_\tau + v_\sigma \partial_x) \Phi_\sigma + \xi(x) e^{i\Phi_\sigma} + \text{c.c.} \right]. \quad (4)$$

The edge conductance G_{ab} can be obtained from the Green function $g_{11}(x, x_0; \omega_n)$ for field Φ_1 via the Kubo formula

$$G_{ab} = \frac{e^2}{h2\pi} \lim_{\omega \rightarrow 0} v \partial_x g_{11}(x, x_0; \omega_n) \Big|_{i\omega_n \rightarrow \omega + i\eta}, \quad (5)$$

where $x_0 < 0$ is in the vicinity of contact a and $x > L$ in the vicinity of contact b . We derive a differential equation for the matrix Green function $\mathbf{g}(x, x_0; \omega_n)$ of fields Φ_1 and Φ_3 from an action analogous to Eq. (1) for $x < 0$ and $x > L$ and the fixed point action Eq. (4) for the region $0 < x < L$. We demand that \mathbf{g} is continuous everywhere and decompose it into a particular part with a discontinuity in its first derivative at $x = x_0$, and a homogeneous part, which is a solution of the differential equations derived from extremizing the actions Eqs. (1) and (4).

III. TRANSPORT-DIFFUSIVE REGIME

We find for the disorder averaged Φ_1 - Φ_1 Green function

$$\bar{g}_{11}(x, x_0; \omega_n) = \frac{2}{3} \frac{2\pi}{\omega_n} \frac{e^{\omega_n(L+x_0-x)/v_1}}{g_\rho(0; \omega_n) - \frac{1}{3}\bar{g}_\sigma(0; \omega_n)} - \frac{\pi}{\omega_n}. \quad (6)$$

Here, g_ρ satisfies the differential equation $(\omega_n + v_\rho \partial_x) g_\rho = 0$ subject to the boundary condition $g_\rho(L, \omega_n) = 1$. In the differential equation for \bar{g}_σ

$$\left(\omega_n + v_\sigma \partial_x - \frac{v_\sigma}{\ell} \right) \bar{g}_\sigma(x; \omega_n) = 0 \quad (7)$$

the nonlinear terms originating from Eq. (4) are replaced by a self-energy term⁶ and the boundary condition $\bar{g}_\sigma(L, \omega_n) = 1$ is imposed. Combining the solution of Eq. (7) with Eqs. (5) and (6), we obtain for the average edge conductance $\bar{G}_{ab} = 2/[3 - \exp(-L/\ell)]$, in agreement with the result in Ref.

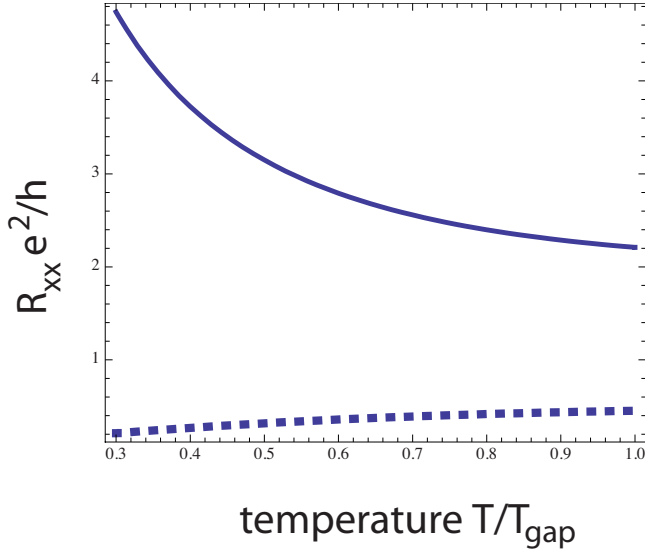


FIG. 3. (Color online) Four terminal resistance due to intraedge scattering for a constriction with $\nu_b=1/3$ and $\nu_c=1/5$ [full line; realizes setup in Fig. 1(a)] and $\nu_c=2/7$ [dotted line; realizes setup in Fig. 1(b)] for $L/\ell_0=3$ and $\Delta=1.5$, from Eq. (9). Increase (decrease) in resistance with decreasing temperature is generic for setup in Fig. 1(a) or 1(b).

11. Neglecting the renormalization of Δ in the range $1 < \Delta < 3/2$, the temperature scaling of the equilibration length is

$$\ell(T) = \ell_0 (T/T_{\text{gap}})^{2-2\Delta}. \quad (8)$$

Here, T_{gap} is the high energy cutoff, which is on the order of the smaller of the two ν_b, ν_c energy gaps. In this simple picture, the equilibration length has the temperature dependence Eq. (8) as long as $L_T < \ell(T)$. The renormalization of disorder stops when L_T exceeds $\ell(T)$, giving rise to a zero-temperature decay length $\ell^* = (\nu_\sigma/T_{\text{gap}})(\ell_0 T_{\text{gap}}/\nu_\sigma)^{1/(3-2\Delta)}$.

In order to make the transition to general ν_b, ν_c , we note that the exponential decay of the neutral mode following from the differential equation Eq. (7) implies an exponential decay of the voltage difference between the two counter-propagating edge states in Fig. 2. Using this insight, a generalization of the average edge conductance to general ν_b, ν_c is possible. We then use the result for the edge conductances \bar{G}_{ab} together with Kirchhoff's laws to obtain the averaged constriction conductance for either of the two geometries of Fig. 1, assuming that the lengths of the two composite edges are equal, and that either L_T or L_V is shorter than L . We find

$$\bar{G}_{12}(T) = \nu_b \nu_c \frac{e^2}{h} \frac{1 \mp e^{-L/\ell(T)}}{\nu_b \pm (\nu_b - 2\nu_c)e^{-L/\ell(T)}}. \quad (9)$$

For setup Fig. 1(a) (upper sign), \bar{G}_{12} decreases with decreasing temperature while for setup Fig. 1(b) (lower sign) it increases with decreasing temperature, see Fig. 3.

IV. COHERENT TRANSPORT

In the regime of coherent transmission $L_T, L_V > L$, the individual realization of disorder determines the conductance.

To calculate the distribution function of the conductance, we once again restrict our considerations to the case of a composite $2/3$ edge or a $1-1/3$ boundary. We make use of the exact solution of the fixed-point Lagrangian Eq. (4) as described in Ref. 6. The neutral part can be mapped onto two copropagating free fermions Ψ_1 and Ψ_2 , where the operator $\partial_x \Phi_\sigma$ corresponds to $\Psi^\dagger \sigma_z \Psi$. The random terms in Eq. (4) can be eliminated by transforming to new fields $\tilde{\Psi}(x) = U(x)\Psi(x)$, with the random SU(2) rotation $U(x)$ defined by

$$U(x) = P \exp \left\{ -i \int_{x_0}^x dx [\xi(x) \sigma^+ + \text{c.c.}] \right\}. \quad (10)$$

Here, P is the path ordering operator and $\sigma^+ = \sigma_x + i\sigma_y$ is a linear combination of two Pauli matrices.

To calculate the exact neutral Green function $g_\sigma(0, L; \omega_n)$, we assume that the random scattering takes place in the region $[0 + \epsilon, L - \epsilon]$. Then, the SU(2) rotation $U(x)$ has no position dependence in a neighborhood of $x=0$ and $x=L$, and we can integrate $\langle \partial_{x_1} \Phi_\sigma \partial_{x_2} \Phi_\sigma \rangle$, which is equal to the exactly known $\langle \Psi^\dagger(x_1) \sigma_z \Psi(x_1) \Psi^\dagger(x_2) \sigma_z \Psi(x_2) \rangle$, with respect to x_1 and x_2 to obtain

$$g_\sigma(0; \omega_n) = \text{Tr}[\sigma_z U(L)^\dagger \sigma_z U(L)] e^{-L\omega_n/\nu_\sigma}. \quad (11)$$

The trace of spin operators on the right-hand side is equal to the cosine of the angle Θ_1 between the original spin quantization axis and the rotated axis. Using this result in an equation for $g_{11}(x, x_0; \omega_n)$ analogous to Eq. (6) but with \bar{g}_σ replaced by $g_\sigma(0; \omega_n)$, we find

$$G_{ab}(\cos \Theta_1) = \frac{e^2}{h} \frac{2}{3 - \cos \Theta_1}. \quad (12)$$

For distances $L \gg \ell$, the rotations $U(L)$ are uniformly distributed over the SU(2) sphere, and $\cos \Theta_1$ is uniformly distributed in $[-1, 1]$. The minimum value $G_{ab}(-1) = e^2/(2h)$ agrees with the minimum conductance found for a model with non-random scattering.¹²

To calculate the conductance of the low-density constriction Fig. 1(a) in the coherent regime, we denote the SU(2) angle of the left composite edge by Θ_1 and the angle for the right composite edge by Θ_2 . If L_T is larger than the composite edge but shorter than the loop around the constriction, interference contributions due to paths winding around the ν_c region can be neglected and

$$G_{12} = \frac{e^2}{h} \frac{(1 - \cos \Theta_1)(1 - \cos \Theta_2)}{3 - \cos \Theta_1 - \cos \Theta_2 - \cos \Theta_1 \cos \Theta_2}. \quad (13)$$

In the limit of adiabatic junctions¹³ with $\cos \Theta_1 = \cos \Theta_2 = -1$, the constriction is fully transparent. For either $\cos \theta_1 = 1$ or $\cos \Theta_2 = 1$ it is fully reflecting.

V. INTEREDGE SCATTERING

Besides the degree of composite edge equilibration, transport through a low-density constriction can be influenced by backwards and forward scattering across the constriction [dashed and dash-dotted lines in Figs. 1(a) and 1(b)]. The relative importance of forward and backwards scattering is

controlled by both the bare tunneling matrix elements and LL renormalization. The bare matrix elements depend in an exponential way on the tunneling distance and are expected to be strongly influenced by the constriction geometry: for a long, “tunnel-like” constriction, backwards scattering may be favored over forward scattering, and for a short constriction, forward scattering may be more important. For a small incompressible region, bare matrix elements may not depend too strongly on the constriction geometry, such that there is a parameter regime, for which renormalization and scaling dimensions may determine the most important tunneling process.

We now consider an idealized model of a square constriction with $L_T \ll L$, such that the bare tunneling matrix elements for competing processes are of comparable size and composite edges are fully equilibrated. We denote the edge creation operator for quasiparticles (QPs) by $\hat{T}(x, t)$ and define its local scaling dimension g by $\langle \hat{T}^\dagger(x, t) \hat{T}(x, 0) \rangle \sim t^{-g}$. The voltage dependence of the scattering probability involving QP operators with scaling dimension g is $\sim V^{-2(1-g)}$, hence the process with the smallest scaling dimension is the most relevant one and will dominate transport in the low energy limit.

On a simple $1/3$ edge, e.g., on the upper and lower edges in Fig. 1(a) with $\nu_b=1$ and $\nu_c=1/3$, and the left and right edges in Fig. 1(b), with $\nu_b=1$ and $\nu_c=2/3$, the operator for $e/3$ QPs is unique and given by $\hat{T}(x, t) = e^{-i\Phi_3(x, t)}$, and its scaling dimension is $g_{\text{simple}} = 1/3$. At a position on the composite edge, e.g., the left or right edge in Fig. 1(a) and top or bottom edge in Fig. 1(b), one has to decompose $\Phi_3 = (\Phi_\sigma - \Phi_\rho)/2$ and has to evaluate the expectation value with respect to the Lagrangian, Eq. (4). One finds $g_{\text{composite}} = 2/3$. There are two other operators with the same scaling dimension, creation of charge $1/3$ QPs by $e^{i(\Phi_\rho + \Phi_\sigma)/2}$ and of charge $2/3$ QPs by $e^{i\Phi_\rho}$. Since $g_{\text{simple}} < g_{\text{composite}}$, scattering between two simple edges is more relevant than scattering between composite edges. Hence, as a function of source-drain voltage, one would expect a zero-bias peak in the differential resistance for the setup in Fig. 1(a) and a zero-bias dip for the setup in Fig. 1(b).

Similarly, a bulk filling factor $\nu_b=1$ and more general constriction fillings from the Jain hierarchy¹⁴ $\nu_n = n/(2n+1)$ with integer n and their particle-hole conjugates can be analyzed. The edge of a $\nu_n = n/(2n+1)$ state flows to a random low-energy fixed point.⁷ This fixed point has one charge mode and $n-1$ neutral modes propagating in the same direction as the charge mode. The most relevant operator for tunneling between two random edges has scaling dimension ν_c and corresponds to a charge ν_c QP. The edge of the particle-hole conjugate states at filling fraction $\nu_n^* = 1 - n/(2n+1)$ flows to a random low-energy fixed point as well,⁷ in this case there is one charge mode and n neutral modes propagating with opposite chirality compared to the charge mode. The most relevant tunneling operator has scaling dimension ν_n^* and corresponds to a QP charge ν_n^* .

A constriction with $\nu_c = \nu_n$ is analogous to the setup Fig. 1(a) with the single-edge mode between constriction and vacuum replaced by n copropagating modes. The most relevant operator for backscattering has scaling dimension ν_c .

The edge between $\nu_c = \nu_n$ and $\nu_b=1$ is equivalent to the edge between ν_n^* and vacuum hence the scaling dimension for forward scattering is $1 - \nu_c$. As $\nu_n < 1/2$, backwards scattering is always more relevant than forward scattering. Next, consider a constriction filling $\nu_c = \nu_n^*$ and bulk filling $\nu_b=1$, which is analogous to the setup in Fig. 1(b). Now, the most relevant operator for backscattering has scaling dimension ν_n^* . The edge between ν_n^* and $\nu_b=1$ is equivalent to an edge between filling fraction ν_n and vacuum, hence the most relevant operator for forward scattering has scaling dimension ν_n , and forward scattering is more relevant than backwards scattering as $\nu_n < \nu_n^*$. In conclusion, for $\nu_c = \nu_n < 1/2$, backscattering across the constriction is more relevant than forward scattering (see table in Fig. 3), and causes a zero-bias peak in the differential resistance. On the other hand, for $\nu_c = \nu_n^* > 1/2$ forward scattering is more relevant and gives rise to a zero-bias dip in the differential resistance, in agreement with the experiments^{3,4} and the particle-hole transformation argument.^{4,5}

Can one expect a similar crossover between peak and dip in the differential resistance for $\nu_b < 1$? An obvious candidate to consider is $\nu_b=1/3$ with constriction filling fractions $\nu_c = 1/5$ and $\nu_c=2/7$. The edge structure of a $\nu_b=1/3$, $\nu_c = 1/5$ constriction is analogous to that of a $\nu_b=1$, $\nu_c=1/3$ constriction, see Fig. 1(a). On the other hand, $\nu_c=2/7$ is an incompressible state of charge $-e/3$ holes and thus analogous to the $2/3$ state, which is an incompressible state of charge $-e$ holes. As a consequence, the edge structure of a $\nu_b=1/3$, $\nu_c=2/7$ constriction is analogous to that of a $\nu_b=1$, $\nu_c=2/3$ constriction, see Fig. 1(b).

The most relevant backwards scattering process between two random $\nu_c=2/7$ edges has scaling dimension $2/7$, whereas the most relevant forward scattering process has scaling dimension $g=3/7$ making backwards scattering more relevant than forward scattering in the case $\nu_c=2/7$. For $\nu_c = 1/5$, backwards scattering is between two simple edges and has a scaling dimension $g=1/5$. The random edge between $\nu_b=1/3$ and $\nu_c=1/5$ can be described by a fixed-point Lagrangian analogous to that in Eq. (4) with the difference that the prefactor multiplying the charge part of the Lagrangian is $15/8\pi$ instead of $3/8\pi$. From this description, we find $g=4/5$ for forward scattering between two of these random edges. As a result, backwards scattering is more relevant than forward scattering in this case as well, and we expect a zero-bias peak in the differential resistance independent of ν_c , in disagreement with the idea of particle-hole conjugation around the metallic state at $\nu_c=1/4$ put forward in Refs. 3 and 5.

What other mechanism besides interedge scattering can explain the experimentally observed crossover³ between a dip in the differential resistance for $\nu_c > 1/4$ and a peak for $\nu_c < 1/4$? As the scaling dimensions for forward and backwards interedge scattering for a $\nu_b=1/3$, $\nu_c=2/7$ constriction are quite similar to each other, it seems plausible that another mechanism with a more pronounced asymmetry between forward and backwards scattering may be dominant. One obvious candidate is the energy dependence of *intraedge* scattering for imperfectly equilibrated composite edges described by Eq. (9). In general, equilibration of composite edges becomes less efficient at low energy, such that

TABLE I. Scaling dimension of the most relevant backward- and forward-scattering operator for a constriction with filling fraction ν_c embedded in a bulk with filling fraction ν_b .

ν_b	ν_c	$g_{\text{backwards}}$	g_{forward}
1	$\frac{2}{3}$	$\frac{2}{3}$	$\frac{1}{3}$
1	$\frac{1}{3}$	$\frac{1}{3}$	$\frac{2}{3}$
1	$\frac{n}{2n\pm 1}$	$\frac{n}{2n\pm 1}$	$1 - \frac{n}{2n\pm 1}$
$\frac{1}{3}$	$\frac{2}{7}$	$\frac{2}{7}$	$\frac{3}{7}$
$\frac{n}{4n-1}$	$\frac{n+1}{4n+3}$	$\frac{n+1}{4n+3}$	$\frac{4n-1}{4n+3}$

upon lowering the energy scale, the resistance increases for setup in Fig. 1(a) and decreases for setup in Fig. 1(b). As illustrated in Fig. 3, this energy dependence can indeed give rise to the experimentally observed zero-bias dip for $\nu_c = 2/7$ and peak for $\nu_c = 1/5$.

In the following, we analyze more examples with $\nu_b > \nu_c > 1/4$ for which backwards scattering is more relevant than forward scattering. Specifically, we choose both $\nu_b = \frac{n}{4n-1}$ and $\nu_c = \frac{n+1}{4(n+1)-1}$ from the Jain sequence.¹⁴ For all n , the edge between ν_c and vacuum has a random low-energy fixed point,⁷ and the scaling dimension of the most relevant scattering operator is ν_c . As the constriction filling fraction is chosen to be one step further in the Jain sequence than the bulk filling fraction, the edge between bulk and constriction has a single-charge mode characterized by the filling fraction difference $\Delta\nu = \nu_b - \nu_c = \frac{1}{(4n-1)(4n+3)}$. The most relevant operator for forward scattering between two $\Delta\nu$ edges has charge $e^* = \frac{e}{4n+3}$ and hence the scaling dimension $(e^*/e\Delta\nu)^2\Delta\nu = \frac{4n-1}{4n+3}$. As this scaling dimension is always larger than the scaling dimension ν_c for backward scattering, we always expect a zero-bias peak in the differential resistance for fully equilibrated edges. Results for the tunneling exponents are summarized in Table I.

VI. CONSTRICTION FILLING $\nu_c = 5/2$

Charge transport through a low-density constriction with $\nu_b = 3$ and $\nu_c = 5/2$ can help to distinguish between two pos-

sible candidates for the $5/2$ FQH state: the Pf and its particle-hole conjugate, the APf,^{9,10} which are topologically different from each other and differ in their edge structure. The scaling dimension for scattering of charge $e/4$ QPs between two Pfaffian edges is $g_{\text{Pf}} = 1/4$, whereas the scattering between two APf edges described by their random fixed point is $g_{\text{APf}} = 1/2$. As the edge between the Pf and $\nu_b = 3$ is equivalent to the edge between APf and $\nu = 2$, in the idealized constriction model the most relevant scattering process for a Pf state in the constriction region is backscattering, causing a zero-bias peak. For an APf state in the constriction on the other hand, the most relevant scattering process is forward scattering, and a zero-bias dip in the differential resistance is expected. If the dominant scattering process is determined by renormalization and not by bare matrix elements, the experiment by Miller *et al.*¹⁵ is evidence for the Pf state to be the preferred ground state for filling fraction $5/2$. However, a recent experiment by Radu *et al.*¹⁶ using samples with a filling fraction $5/2$ in both the bulk and the constriction region is best described by a tunneling exponent $g_{\text{APf}} = 1/2$.

VII. SUMMARY

In conclusion, we have discussed how the presence of composite edges around a low-density constriction influences transport in important ways. For a constriction in the diffusive regime, incomplete equilibration of composite edges gives rise to a voltage and temperature dependence of the conductance. Even more strikingly, in the limit of coherent transport through composite edges, we predict universal conductance oscillations and calculate their full distribution function. The LL renormalization of interedge scattering across the constriction region determines whether the most relevant scattering process is forward or backwards scattering.

ACKNOWLEDGMENTS

Work was supported by NSF under Grant No. DMR 0906475 and by the Heisenberg program of DFG.

¹X. G. Wen, *Phys. Rev. B* **44**, 5708 (1991); *Phys. Rev. Lett.* **64**, 2206 (1990).

²Y. C. Chung, M. Heiblum, and V. Umansky, *Phys. Rev. Lett.* **91**, 216804 (2003).

³S. Roddaro, V. Pellegrini, F. Beltram, G. Biasiol, and L. Sorba, *Phys. Rev. Lett.* **93**, 046801 (2004).

⁴S. Roddaro, V. Pellegrini, F. Beltram, L. N. Pfeiffer, and K. W. West, *Phys. Rev. Lett.* **95**, 156804 (2005).

⁵S. Lal, *EPL* **80**, 17003 (2007); *Phys. Rev. B* **77**, 035331 (2008).

⁶C. L. Kane, M. P. A. Fisher, and J. Polchinski, *Phys. Rev. Lett.* **72**, 4129 (1994).

⁷C. L. Kane and M. P. A. Fisher, *Phys. Rev. B* **51**, 13449 (1995).

⁸C. Nayak, S. H. Simon, A. Stern, M. Freedman, and S. Das Sarma, *Rev. Mod. Phys.* **80**, 1083 (2008).

⁹S.-S. Lee, S. Ryu, C. Nayak, and M. P. A. Fisher, *Phys. Rev. Lett.* **99**, 236807 (2007).

¹⁰M. Levin, B. I. Halperin, and B. Rosenow, *Phys. Rev. Lett.* **99**, 236806 (2007).

¹¹D. Sen and A. Agarwal, *Phys. Rev. B* **78**, 085430 (2008).

¹²V. V. Ponomarenko and D. V. Averin, *Phys. Rev. Lett.* **97**, 159701 (2006); this disagrees with U. Zülicke and E. Shimshoni, *ibid.* **97**, 159702 (2006).

¹³D. B. Chklovskii and B. I. Halperin, *Phys. Rev. B* **57**, 3781 (1998).

¹⁴J. K. Jain, *Phys. Rev. Lett.* **63**, 199 (1989).

¹⁵J. B. Miller, I. P. Radu, D. M. Zumbuhl, E. M. Levenson-Falk, M. A. Kastner, C. M. Marcus, L. N. Pfeiffer, and K. W. West, *Nat. Phys.* **3**, 561 (2007).

¹⁶I. P. Radu, J. B. Miller, C. M. Marcus, M. A. Kastner, L. N. Pfeiffer, and K. W. West, *Science* **320**, 899 (2008).